ACS APPLIED MATERIALS & INTERFACES

Research Article

www.acsami.org

Amperometric Detection of Lactose Using β-Galactosidase Immobilized in Layer-by-Layer Films

Paula P. Campos,[†] Marli L. Moraes,[‡] Diogo Volpati,[§] Paulo B. Miranda,[§] Osvaldo N. Oliveira, Jr.,[§] and Marystela Ferreira*[,†]

[†]Federal University of São Carlos, UFSCar, Campus Sorocaba, Rodavia João Leme dos Santos, km 110 - SP-264, São Carlos SP, 18052-780 Brazil

[‡]Instituto de Ciência e Tecnologia, Federal University of São Paulo, Unifesp, Campus São José dos Campos, Rua Talim, 330, São José dos Campos SP, 12231-280 Brazil

[§]São Carlos Institute of Physics, University of São Paulo, Av. Trabalhador São-carlense, 400, São Carlos SP, 13560-970 Brazil

Supporting Information

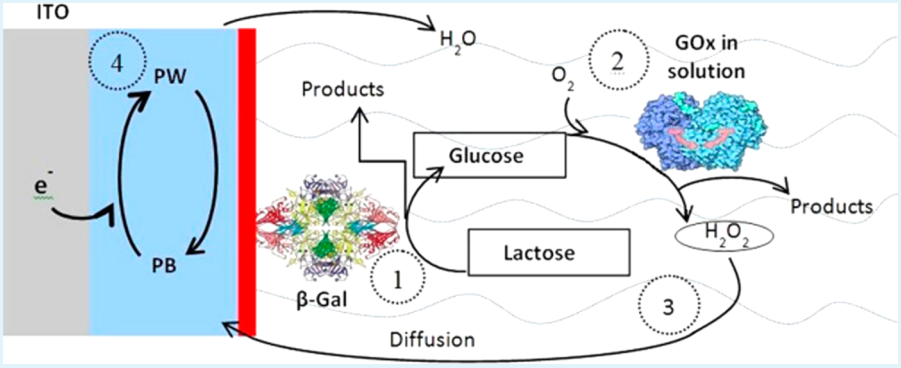

ABSTRACT: A direct, low-cost method to determine the concentration of lactose is an important goal with possible impact in various types of industry. In this study, a biosensor is reported that exploits the specific interaction between lactose and the enzyme β-galactosidase (β-Gal) normally employed to process lactose into glucose and galactose for lactose-intolerant people. The biosensor was made with β-Gal immobilized in layer-by-layer (LbL) films with the polyelectrolyte poly(ethylene imine) (PEI) and poly(vinyl sufonate) (PVS) on an indium tin oxide (ITO) electrode modified with a layer of Prussian Blue (PB). With an ITO/PB/$(PEI/PVS)_1(PEI/\beta\text{-Gal})_{30}$ architecture, lactose could be determined with an amperometric method with sensitivity of 0.31 μA $mmol^{-1}$ cm^{-2} and detection limit of 1.13 mmol L^{-1}, which is sufficient for detecting lactose in milk and for clinical exams. Detection occurred via a cascade reaction involving glucose oxidase titrated as electrolytic solution in the electrochemical cell, while PB allowed for operation at 0.0 V versus saturated calomel electrode, thus avoiding effects from interfering species. Sum-frequency generation spectroscopy data for the interface between the LbL film and a buffer containing lactose indicated that β-Gal lost order, which is the first demonstration of structural effects induced by the molecular recognition interaction with lactose.

KEYWORDS: *lactose, amperometric detection, β-galactosidase, layer-by-layer, sum-frequency generation*

INTRODUCTION

Lactose, a disaccharide found in milk and dairy products, is the only source of carbohydrates in milk, with concentrations ranging from 4.4 to 5.2%.[1] It is hydrolyzed by lactase in the digestive system to the monosaccharides glucose and galactose. For humans suffering from lactose intolerance for the lack of lactase, the commercially available β-galactosidase may be used to hydrolyze lactose to be absorbed by the body. Lactose concentrations may be indicative of abnormalities and be used for clinical diagnosis. For instance, lactose in excess in the blood indicates gastrointestinal malignancy.[2] The quantitative determination of lactose is usually performed in specialized laboratories, and requires long analysis times and expensive instruments for methods such as spectrophotometry,[3] infrared spectroscopy,[4] titrimetry,[5] and chromatography.[6,7]

The development of a low-cost, fast method for monitoring lactose is therefore an important aim, which may be achieved with biosensors based on an enzymatic cascade reaction with β-galactosidase (β-Gal) in the presence of glucose oxidase (GOx).[8,9] In these biosensors β-Gal catalyzes the hydrolysis of lactose, producing glucose, which is catalyzed by GOx, thus generating hydrogen peroxide (H_2O_2). Examples include an

Received: April 22, 2014
Accepted: July 3, 2014
Published: July 3, 2014

amperometric biosensor with β-Gal, GOx, peroxidase (HRP), and the mediator tetrathiafulvalene (TTF) coimmobilized onto a gold electrode modified by a self-assembled monolayer (SAM).[2] Detection was carried out at 0.00 V (vs Ag/AgCl) with the signal being proportional to the lactose concentration between 1.5 and 120 μmol L^{-1}. Another amperometric biosensor was prepared by immobilizing β-Gal and GOx with glutaraldehyde onto a glassy carbon electrode coated with a mercury thin film.[10]A spectrophotometric assay for quantifying lactose was developed with β-Gal, GOx, HRP, and *o*-phenylenediamine (OPD) for the concentration range from 0.2 to 1.8 mmol L^{-1}.[11]

In this study, we also exploit β-galactosidase, but immobilized with the layer-by-layer (LbL) technique together with the polyelectrolyte PEI onto an indium tin oxide (ITO) electrode modified with Prussian Blue (PB), which served as mediator for H_2O_2.[12] GOx was incorporated into the electrolyte solution. The design of this biosensor has advantages over those reported in the literature, which include a suitable enzyme immobilization method;[13] only two enzymes are involved in the cascade reaction and the oxidation of H_2O_2 is carried out at 0.0 V (vs SCE).[14] The choice of the LbL method was based on its suitability to immobilize enzymes with preserved activity.[15−19] PEI was selected because it has been proven more adequate than other polyelectrolytes for preserving enzyme activity.[12,20,21] We also performed sum-frequency generation (SFG) measurements in an attempt to correlate the detection of lactose with changes in the immobilized β-galactosidase.

EXPERIMENTAL SECTION

Materials. The enzyme β-galactosidase (β-Gal) (E.C. 3.2.1.23) from *Aspergillus oryzae*, isoelectric point at pH 4.6, optimal activity between pH 4.5 and 5[22] and 8 units/mg; glucose oxidase (GOx) from *Aspergillus niger* (E.C. 1.1.3.4), isoelectric point at pH 4.2,[23] optimal activity between pH 3.5 and 6.5[24] and 138.8 units/mg; poly(ethylene imine) (PEI), poly(vinyl sufonate) (PVS), β-lactose, glucose, and sucrose were purchased from Sigma-Aldrich; ascorbic acid was purchased from Cinética, and uric acid was obtained from Fluka.

Substrate. The LbL films were assembled onto quartz slides and CaF_2 plates for spectroscopic investigations and onto ITO-coated glass (one side coated on glass by Delta Technologies) for electrochemical measurements. The quartz plates were cleaned with $HCl/H_2O_2/H_2O$ (1:1:6) (v/v) and $NH_4OH/H_2O_2/H_2O$ (1:1:5) (v/v) hydrophilization solutions, both for 10 min at 80 °C, while CaF_2 windows were cleaned with hydrogen peroxide and potassium permanganate. The ITO was cleaned with chloroform, isopropanol (in a sonicator), and rinsed with ultrapure water (Milli-Q). ITO slides were previously modified with a Prussian Blue (PB) layer.[25]

Solutions. The solutions of PEI (1 mg mL^{-1}) were prepared in ultrapure water with pH adjusted to 5.5 by adding HCl (1 mol L^{-1}). The solutions of PVS (4 μL mL^{-1}), GOx (0.5 mg mL^{-1}), β-Gal (5 mg mL^{-1}), lactose (1 mol L^{-1}), glucose (1 mol L^{-1}), sucrose (1 mol L^{-1}), ascorbic acid (1 mol L^{-1}), and uric acid (10 mmol L^{-1}) were prepared in a sodium acetate buffer (0.05 mol L^{-1}, pH 5.5). The molecular weights were Mw = 200 000−350 000 for PVS and Mw = 750 000 for PEI.

LbL Films. For fluorescence and optical absorption measurements, 2-bilayer $(PEI/PVS)_2$ LbL films were used as a cushion to reduce the influence of substrate morphology on film growth,[26] while the amperometric measurements were made with a 1-bilayer cushion of $(PEI/PVS)_1$. LbL films were assembled by dipping the substrate in PEI and β-Gal solutions, both for 3 min, interspersing the immersion in sodium acetate buffer during 30 s for washing. This procedure was repeated until the desired number of bilayers was reached. Film growth was monitored by measuring the fluorescence spectrum at each bilayer deposited with a Thermo Scientific Shimadzu model RF-5301 PC spectrofluorimeter. The absorption spectra were taken with a Thermo Scientific Genesys 6 UV−vis spectrophotometer. All the films were assembled at room temperature. For Fourier transform infrared (FTIR) and SFG spectroscopic measurements, a 2-bilayer cushion of $(PEI/PVS)_2$ was deposited onto the CaF_2 windows, on top of which one bilayer of $(PEI/\beta\text{-Gal})_1$ was added, leaving the β-Gal exposed in the outermost layer.

Electrochemical Measurements. The PB film was potentiostatically deposited onto ITO at a potential of +0.40 V (vs Ag/AgCl electrode) during 400 s from aqueous 2×10^{-3} mol L^{-1} $K_3[Fe(CN)_6]$ + 2×10^{-3} mol L^{-1} $FeCl_3$ solutions in 0.1 mol L^{-1} KCl + 0.01 mol L^{-1} HCl. After deposition, the modified electrodes were rinsed with Milli-Q water and immersed into a solution containing 0.1 mol L^{-1} KCl + 0.01 mol L^{-1} HCl, where the electrode potential was cycled between 0.0 and 1.0 V (vs Ag/AgCl electrode) at a scan rate of 0.05 V s^{-1}, until a stable voltammetric response was obtained.[12] Amperometric measurements were performed at 0.0 V versus saturated calomel electrode (SCE) with an Autolab PGSTAT 30 using a conventional electrochemical cell (7 mL of sodium acetate buffer + 500 μL of GOx), comprising an auxiliary electrode of platinum foil (1 cm^2) and the working electrodes being ITO modified with LbL films with a PB layer as follows: $ITO/PB/(PEI/PVS)_1(PEI/\beta\text{-Gal})_{10}$ or $ITO/PB/(PEI/PVS)_1(PEI/\beta\text{-Gal})_{30}$. The applied potential for each biosensor was kept at 0.0 V allowing the background current to decay to a steady state value before the amperometric experiments in each addition of lactose (100 μL, 0.1 mol L^{-1}) under stirring. Usually, 1 min elapsed before the measurements were taken, to get a stable signal. The effect from interferents and the stability of the biosensor were also studied.

FTIR and SFG Spectroscopy Studies. The FTIR spectra were acquired in N_2-purged atmosphere using a Nicolet 470 Nexus spectrometer. In the experiments with the enzyme powder, 0.5% of β-Gal was dispersed in pellets in a KBr matrix. For the measurements on films, $(PEI/PVS)_3$ and $(PEI/PVS)_2$+$(PEI/\beta\text{-Gal})_1$ LbL films were grown onto CaF_2 windows and then dried in a weak flow of N_2. All measurements were carried out in the transmission mode with a resolution of 6 cm^{-1}.

The SFG spectroscopy measurements were performed on the upper face of a CaF_2 plate at a film−air interface, on which LbL films were grown with the enzyme immobilized. The film architectures investigated were $(PEI/PVS)_3$ and $(PEI/PVS)_2$+$(PEI/\beta\text{-Gal})_1$, which were exposed to buffer or lactose solutions and then dried in a low flux of N_2 before the experiments. The setup consists of two laser beams, one in the visible range (ω_{vis}) and another, tunable in the infrared (ω_{IR}), both overlapping spatially and temporally at the interface giving rise to a sum-frequency signal $\omega_{SFG} = \omega_{vis} + \omega_{IR}$. When the IR beam frequency matches a normal vibration mode, the intensity of the SFG signal increases. However, if the molecules at the interface have a null or random orientation, the SFG signal is zero. Therefore, even the molecules at the interface must have a net average orientation to obtain a measurable SFG signal. Scheme 1 displays an idealized structure of the samples analyzed by SFG spectroscopy.

For the analysis of the vibrational spectrum, the intensity of the SFG signal may be expressed as

$$I_{SFG} \propto |\chi^{(2)}_{eff}|^2 = |\chi^{(2)}_{NR} + \chi^{(2)}_{R}|^2 = \left|\chi^{(2)}_{NR} + N_S \sum_q \frac{A_q}{\omega_{IR} - \omega_q + i\Gamma_q}\right|^2 \quad (1)$$

where $\chi^{(2)}_{NR}$, $\chi^{(2)}_{R}$, N_s, A_q, ω_q, Γ_q are the nonresonant and resonant contributions to $\chi^{(2)}_{eff}$, the surface density of molecules and, respectively, the oscillator strength, resonant frequency and line width of vibrational mode *q*. From eq 1 one notes that when ω_{IR} is near the frequency of molecular vibrations ω_q, the SFG output is resonantly enhanced. Equation 1 also illustrates a feature of nonlinear spectroscopic methods that differ from their linear counterparts: there is *interference* of the resonant contribution, $\chi^{(2)}_{R}$, with the nonresonant background, $\chi^{(2)}_{NR}$, leading to changes in the spectral line shape depending on both

Scheme 1. Structure of a 2-Bilayer $(PEI/PVS)_2$ LbL Film[a]

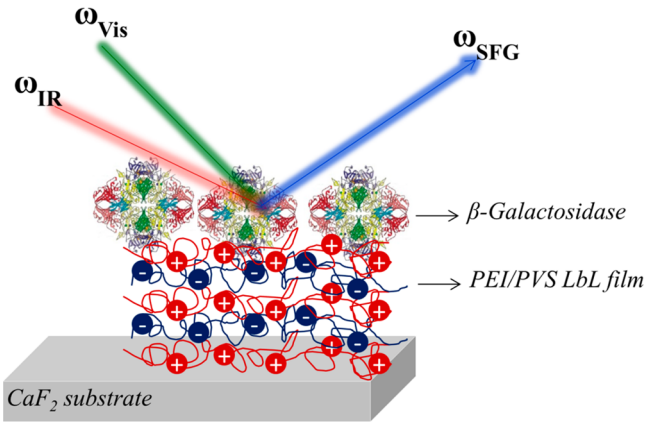

[a] The enzyme β-galactosidase was immobilized with a top $(PEI/\beta\text{-Gal})_1$ bilayer on the LbL film. The laser beams ω_{vis} and ω_{IR} overlap spatially and temporally to generate the SFG signal $\omega_{SFG} = \omega_{vis} + \omega_{IR}$.

the magnitude and phase of $\chi^{(2)}_{NR}$ and on the presence of nearby resonances. Therefore, a quantitative analysis of SFG spectra requires curve fitting to eq 1 to obtain the amplitudes, frequencies, and line widths of the resonances. Further details on the SFG technique are available in refs 27 and 28.

The SFG vibrational spectra were obtained with a commercial spectrometer (Ekspla, Lithuania) equipped with a pulsed Nd^{3+}:YAG laser that provides a fundamental beam at 1064 nm (28 ps pulse duration, 20 Hz repetition rate) with a harmonic unit generating second and third harmonics (532 and 355 nm, respectively). The third harmonic and fundamental beams pump an optical parametric amplifier with a difference frequency stage that generates an infrared (IR) beam tunable from 1000 to 4000 cm^{-1} with pulse energy ~30–200 μJ. The spot sizes and incidence angles for the IR and visible (532, 600 μJ) beams are 0.50 mm, 55° and 1.00 mm, 60°, respectively. The SFG signal is measured with a photomultiplier after spatial and spectral filtering, with data being collected for each scan with 100 shots data point, with a resolution of 3 cm^{-1}. The molecular-level information was obtained by analyzing the SFG measurements in *ppp* polarization combinations (*p* sum-frequency generated beam, *p* visible beam, and *p* IR beam).

RESULTS AND DISCUSSION

Electrode Preparation. Scheme 2 shows the idealized structure of an LbL film containing the immobilized enzyme onto ITO modified with a PB layer and also includes the mechanisms for detection of lactose. This is carried out in the presence of GOx in the buffer solution, with generation of H_2O_2, as depicted in steps 1, 2, 3, and 4 in Scheme 2.

PB films can be reduced to their colorless form, referred to as Prussian White (PW), according to eq 2:

$$KFe^{III}Fe^{II}(CN)_6 + e^- + K^+ \rightarrow K_2Fe^{II}Fe^{II}(CN)_6 \qquad (2)$$

where Fe^{III} and Fe^{II} are the oxidation states of Fe atoms in the PB structure.[12,29] In subsidiary experiments we observed that bare ITO and ITO modified with PB used in amperometric measurements failed to detect lactose.

Film Growth. The absorbance spectra for β-Gal in solution and immobilized in a PEI/β-Gal8-bilayer LbL film in Figure 1A

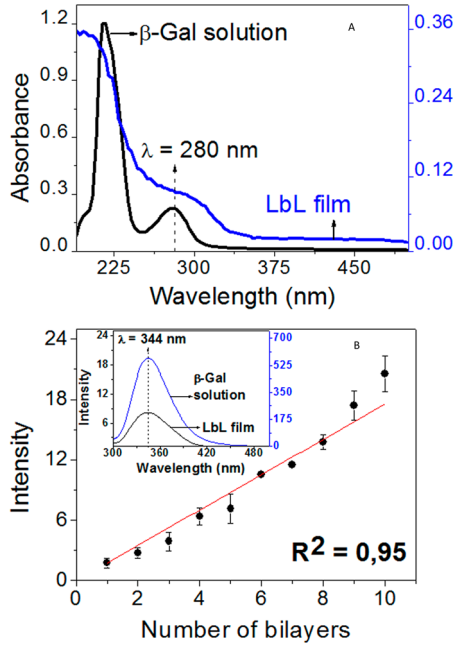

Figure 1. (A) Absorption spectrum for β-Gal in sodium acetate buffer at pH 5.5 and in LbL films. (B) Fluorescence intensity vs number of bilayers for a $(PEI/PVS)_2(PEI/\beta\text{-Gal})_{10}$ LbL film at 344 nm and with excitation at 280 nm. (inset) The emission spectra for β-Gal in sodium acetate buffer at pH 5.5 and in an LbL film.

display absorption bands at λ = 215 and 280 nm, assigned to tryptophan, phenylalanine, and tyrosine and peptide bonds, which confirm the enzyme immobilization. Film growth was successful with the same amount deposited in each deposition

Scheme 2. Biosensor Made with a $(PEI/\beta\text{-Gal})_n$ LbL Film Operating at 0.0 V vs SCE

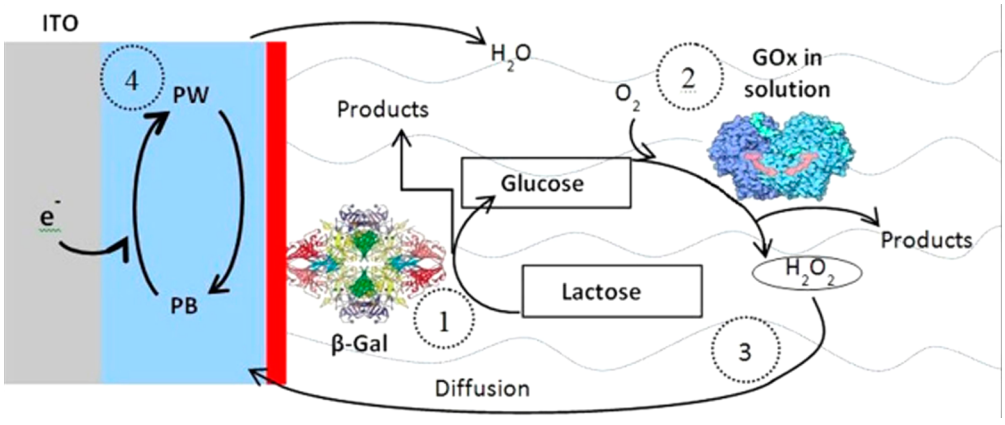

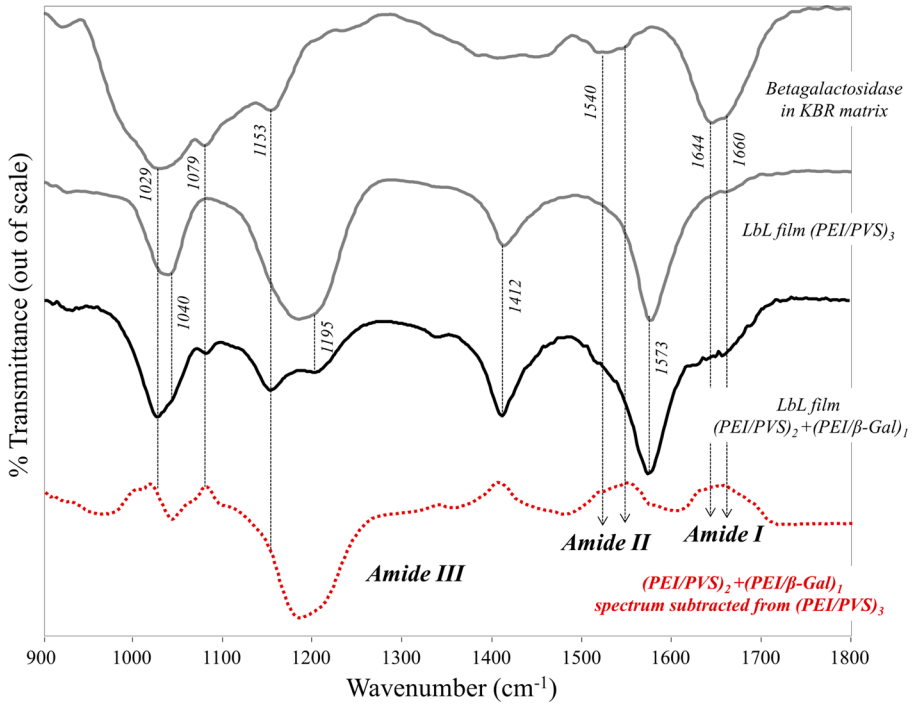

Figure 2. FTIR absorption spectra for β-Gal in KBr pellet and for LbL films of $(PEI/PVS)_3$ and $(PEI/PVS)_2$+$(PEI/\beta\text{-gal})_1$. The red dotted spectrum was obtained by subtracting the $(PEI/PVS)_2$+$(PEI/\beta\text{-gal})_1$ spectrum from that of $(PEI/PVS)_3$, which reveals the main bands of the enzyme immobilized in the film. The LbL films were grown onto a CaF_2 plate up to three bilayers.

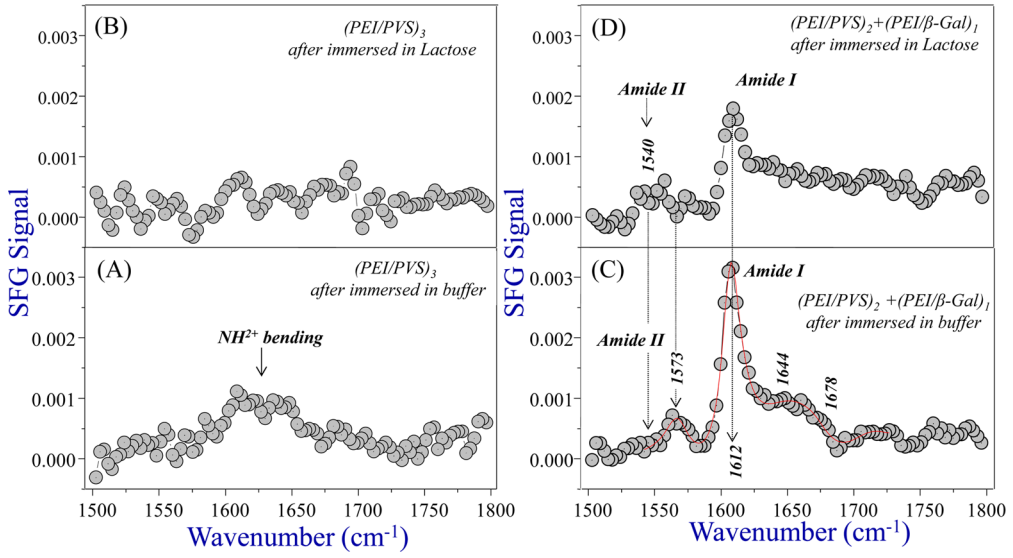

Figure 3. SFG spectra for the samples $(PEI/PVS)_3$ (A) after contact with buffer solution and (B) lactose solutions, and $(PEI/PVS)_2$+$(PEI/\beta\text{-Gal})_1$ (C) after contact with buffer solution and (D) lactose solution. The measurements were performed in a *ppp* polarization configuration. The spectrum in figure (C) is fitted to eq 1, illustrated by a red line, and the bands are highlighted.

step, as indicated by the linear increase in the fluorescence intensity at 344 nm for $(PEI/PVS)_2(PEI/\beta\text{-Gal})_1$ LbL films in Figure 1B, with excitation at 280 nm. Emission at 344 nm is attributed to phenylalanine, tyrosine, and tryptophan chromophores in the enzyme.[30] Absorption spectra shown in the Supporting Information confirmed the success of the LbL deposition.

FTIR and SFG. The FTIR spectrum for β-Gal dispersed in a KBr matrix in Figure 2 exhibits the main bands of the enzyme, which are consistent with the literature.[31] The bands at 1650 and 1540 cm^{-1} are assigned to the amides I and II, respectively.[32−35] The doublet at 1644 and 1660 cm^{-1} in the amide I region allows one to probe the enzyme structure, since the former is associated with *β-sheets* or *random coils*, while the latter at 1660 cm^{-1} is related to *α-helices*.[31,34,36,37]

The main bands for $(PEI/PVS)_3$ LbL films in Figure 2 appear at 1040, 1195, 1412, and 1573 cm^{-1}, assigned to the symmetric and asymmetric stretching of SO groups, angular deformations of CH (bending) in the polymer chains, and angular deformation of NH groups, respectively.[38−40] Since SO and NH groups are related to PVS and PEI, respectively, the spectra confirm the presence of these two polyelectrolytes in

the $(PEI/PVS)_3$ LbL films. The spectrum for the $(PEI/PVS)_2$+$(PEI/\beta\text{-Gal})_1$ LbL film exhibited the same bands observed for β-Gal and PEI/PVS film, with no band shifts or appearance of additional bands. The main bands of β-Gal, namely, amides I and II and III, are inferred in the LbL film from spectral subtraction of $(PEI/PVS)_3$ and $(PEI/PVS)_2$+$(PEI/\beta\text{-Gal})_1$, especially for amide III band that is overlapped by the $(PEI+PVS)_3$ bands at ca. 1200 cm^{-1}. Therefore, there is no strong molecular-level interaction between the film components, in spite of the high stability of the enzyme in the film when exposed to aqueous media. This stability should be governed by electrostatic interactions and H-bonding between the PEI/PVS film and β-Gal, which are usually the main driving forces for film growth.[41,42]

Molecular organization in the $(PEI/PVS)_3$ LbL film after being immersed into the buffer solution is weak according to the SFG spectrum in Figure 3A, where only a broad, low-intensity band appeared between 1600 and 1650 cm^{-1}, assigned to the angular deformation of NH^{2+} group as an ionized form of the polymer when in the water.[39,43] When this $(PEI/PVS)_3$ LbL film was immersed in a lactose solution, even the weak signal practically disappeared as indicated in Figure 3B.

The adsorption of an enzyme layer brought considerable molecular organization, as is clear from the spectrum in Figure 3C for the $(PEI/PVS)_2$+$(PEI/\beta\text{-Gal})_1$ LbL film after being immersed in the buffer solution. Four bands could be identified when the spectrum was fitted to eq 1, at 1573, 1612, 1644, and 1678 cm^{-1}. The peak at 1573 cm^{-1} is assigned to a PEI vibrational mode and was also observed in the FTIR results. Since this mode was not present in the spectrum for the $(PEI/PVS)_3$ film, one infers that it becomes active in SFG owing to interactions with the enzyme, thus adopting a net orientation in the outer polymer layer. The bands at 1644 and 1678 cm^{-1} are attributed to *β-sheets* and *β-turns* of the enzyme, respectively.[36,31,34] The most intense peak at 1612 cm^{-1} is also assigned to the enzyme; according to the literature it can either be due to *aggregate strands* or *β-sheets* induced by intermolecular enzyme interactions.[44,45,34] The conformation inferred for the enzyme does not coincide with that found via FTIR measurements (KBr pellet), which could be due to two main reasons: in the KBr pellet the enzyme would adopt a different conformation and/or the enzyme structure was modified upon immobilization on the LbL film. However, CD measurements (see Supporting Information) indicate only a small conformational change of the enzyme upon immobilization onto the PEI layer. This suggests that the conformation dominant in the SFG spectrum is not the most abundant in the protein, but rather the most well-oriented in the adsorbed enzyme.

The effect from exposing the $(PEI/PVS)_2$+$(PEI/\beta\text{-Gal})_1$ LbL film to lactose was considerable, as shown in Figure 3D. The decrease in the band intensities points to a much less-ordered film than when exposing the film to the buffer only (no lactose). Therefore, lactose appears to have a disordering effect on the LbL films. This applies to the neat $(PEI/PVS)_3$ film, but especially for the film containing the enzyme, as is seen for the amide I band. To our knowledge, this is the first observation of such disordering effect caused by lactose. We do not know whether this is specific for the lactose−galactosidase interaction, since the initial order of LbL films can also be altered by other factors such as a flux of air,[46] heating,[46,47] or exposure to specific vapors.[48]

Amperometric Measurements. The amperometric response of LbL films containing β-Gal was tested, and the results are shown in Figures 4 and 5 for biosensors with the architecture ITO/PB/$(PEI/PVS)_1(PEI/\beta\text{-Gal})_n$ with 10 and

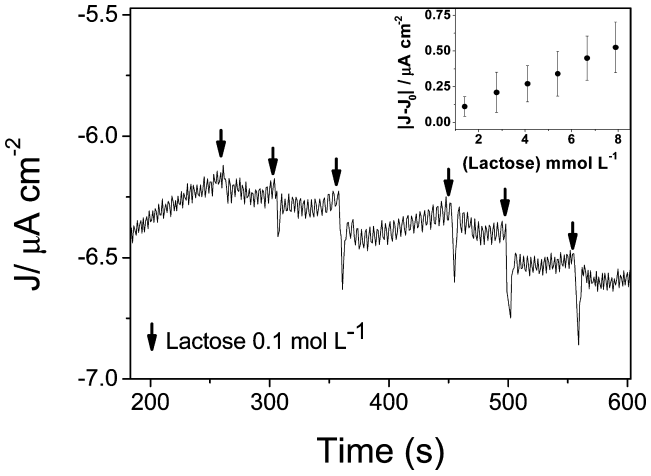

Figure 4. Amperometric response of biosensor ITO/PB/$(PEI/PVS)_1(PEI/\beta\text{-Gal})_{10}$ in sodium acetate buffer pH 5.5 and GOx. (inset) Current density as a function of lactose concentration.

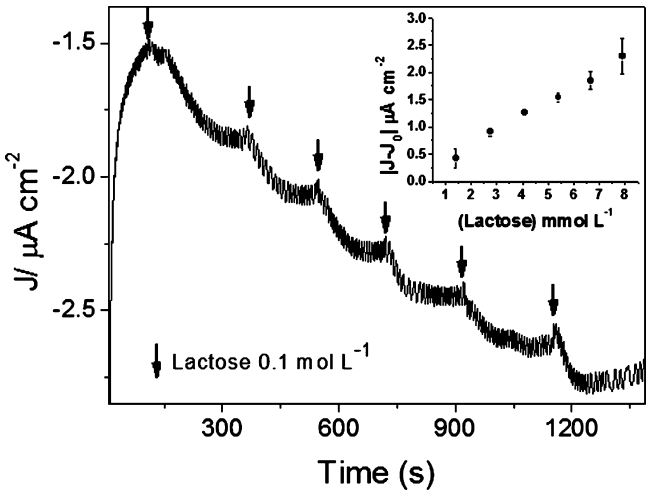

Figure 5. Amperometric response of biosensor ITO/PB/$(PEI/PVS)_1(PEI/\beta\text{-Gal})_{30}$ in sodium acetate buffer pH 5.5 and GOx. (inset) Current density versus lactose concentration.

30 bilayers (n is the number of PEI/β-Gal bilayers), respectively, operating at 0.0 V (vs SCE) in a sodium acetate buffer and GOx solution at pH 5.5. The biofunctionality of β-Gal/PEI LbL structure as well as the feasibility of the method for biosensing are demonstrated by the increase in reduction current upon addition of successive aliquots of lactose. Each addition corresponds to an increase of 100 μL of 1×10^{-1} mol L^{-1} lactose in 7 mL of sodium acetate buffer of supporting electrolyte.

A stronger response was obtained for the biosensor made with the 30-bilayer LbL film in Figure 5, with a clear signal transduction for detecting the lactose aliquots. Figure 6 shows the analytical curves for ITO/PB/$(PEI/PVS)_1(PEI/\beta\text{-Gal})_n$ biosensors, with n = 10 and 30. The sensitivity, inferred from the slope of the fitted curve,[47] increased with the number of bilayers, probably owing to the larger amount of β-Gal immobilized. The sensitivity achieved in the biosensors with a linear response was 0.064 and 0.31 μA $mmol^{-1}$ cm^{-2} lactose,

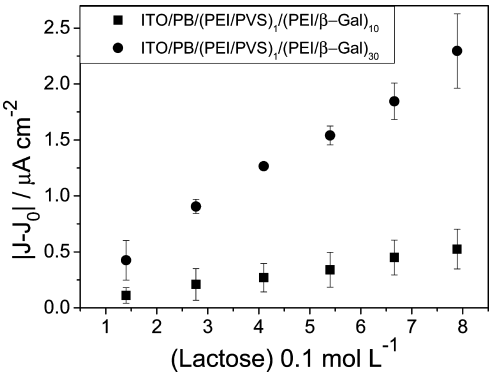

Figure 6. Linear range of analytical curves extracted from LbL films with 10 and 30 bilayers.

respectively. The apparent Michaelis–Menten constant[49] was determined as being 8.26 mmol L^{-1} and 8.24 mmol L^{-1} for the 10- and 30-bilayer LbL films, respectively, to be compared with 1.31 mmol L^{-1}[50] and 1.25 mmol L^{-1}[51] for the free enzyme. The values for the LbL films are similar to reports in the literature, for example, 5.18 mmol L^{-1}[52] and 5.2 mmol L^{-1},[53] but one must consider that the film architectures differed or the films were fabricated with other methods.

The limit of detection for the biosensors was 4.22 mmol L^{-1} for ITO/PB/$(PEI/PVS)_1(PEI/\beta\text{-Gal})_{10}$ and 1.13 mmol L^{-1} for ITO/PB/$(PEI/PVS)_1(PEI/\beta\text{-Gal})_{30}$. The PEI/$\beta$-Gal-based biosensor displayed a larger limit of detection than others reported in the literature, according to Table 1, but its sensitivity is still sufficient to detect lactose in commercial milk. Indeed, the lactose concentration in pure milk is typically on the order of 100 mmol L^{-1},[54] which is 100-fold our limit of detection.

Table 1. Biosensors for Detecting Lactose

authors	method of detection[a]	limit of detection (mmol L^{-1})
Conzuelo, F.; Gamella, M.; Campuzano, S.; Ruiz, M. A.; Reviejo, A. J.; Pingarrón, J. M., 2010	amperometric	4.6×10^{-4}
Fornera, S.; Yazawa, K.; Walde, P., 2011	spectrometric	0.10
Göktuğ, T.; Sezgintürk, M. K.; Dinçkaya, E., 2005	amperometric	0.58
this work	amperometric	4.22 and 1.13

[a]The spectrometric method is based on the color change while the amperometric method uses the change in current as a function of time with a fixed applied potential.

The successful detection of lactose implies that β-Gal had its activity (and therefore structure) preserved in the PEI/β-Gal LbL films. We confirmed with circular dichroism (CD) measurements reported in the Support Information that immobilization of β-Gal in PEI/β-Gal LbL films led to a small loss of α-helices (from 74 to 69%) compared to the enzyme free in solution. This is in contrast to the much more extensive denaturing of β-Gal in LbL films with poly(allylamine hydrochloride) (PAH), which is also indicated in the Supporting Information. Therefore, the choice of PEI for building the LbL films was justified. We also tried to detect lactose using amperometry with LbL films containing the two enzymes, namely, β-Gal and GOx immobilized in the same film, but the results were poor, probably because the active sites of one of the enzymes was blocked.

Effects from Interferents. Effects from interferents represent the major difficulty for a biosensor in real applications. With the architecture used here, comprising a PB layer under the LbL films, detection was performed at 0.0 V versus SCE, which helped prevent interferent effects. This is demonstrated in the results of Figure 7, from experiments where the unbiased electrode ITO/PB/$(PEI/PVS)_1(PEI/\beta\text{-Gal})_{30}$ (0.0 V vs SCE) were first subjected to 0.1 mol L^{-1} lactose solution until the current reached a steady-state value, and then successive injections of interferents were made, as indicated by arrows. The interferents caused no detectable change in current, with the exception of ascorbic acid, which made the current increase rather than decrease as occurs for lactose. Therefore, though ascorbic acid gives a signal, it can still be distinguished from lactose, highlighting the specificity of the biosensor. As expected, glucose made the current decrease, which could seem to compromise the ability to detect lactose. However, this can be circumvented with a glucose biosensor coupled to the lactose biosensor, for the concentration of lactose would be the difference in the signal.

Biosensor Stability. The stability of the biosensors was investigated in terms of their performance for discriminating lactose. The biosensors were stored in sodium acetate buffer (pH 5.5) at 10 °C when not in use. For the ITO/PB/$(PEI/PVS)_1(PEI/\beta\text{-Gal})_{30}$ system, the response was unaltered for 12 d, after which the signal decreased. All measurements were made in duplicate, and the stability tests confirmed the film reproducibility.

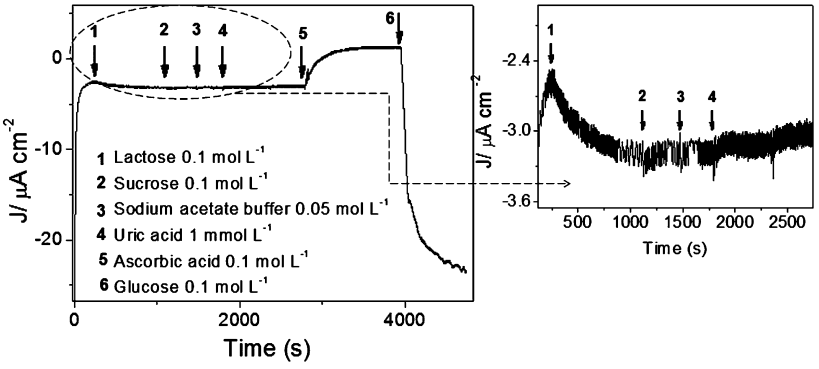

Figure 7. Tests with interferents, titration 100 μL of (1) lactose 0.1 mol L^{-1}, (2), sucrose 0.1 mol L^{-1}, (3) sodium acetate buffer 0.05 mol L^{-1}, (4) uric acid 1 mmol L^{-1}, (5) ascorbic acid 0.1 mol L^{-1}, (6) glucose 0.1 mol L^{-1}.

CONCLUSIONS

The LbL technique was proven suitable for immobilizing β-Gal, with LbL films deposited on a PB-modified ITO electrode being used for detecting lactose. The amperometric biosensor was not as sensitive as similar ones in the literature, but its sensitivity is sufficient for detecting lactose in actual applications, especially as it has been proven robust against interferents and displayed a stable performance over time. Moreover, the molecular architecture of the biosensor allows for further developments in terms of optimizing performance and being amenable to miniaturization for point-of-care use.

In addition to confirming the successful adsorption of β-Gal in the LbL films, SFG vibrational spectroscopy was useful to indicate that sensing lactose is accompanied by a decrease in the orientational order of the immobilized enzymes. This appears to be the first observation ever of molecular rearrangements induced by lactose detection, and it opens the way for the identification of intermolecular interactions responsible for biosensing. It is also a first step toward understanding the mechanism of molecular recognition, which is crucial for any biological application.

ASSOCIATED CONTENT

Supporting Information

The LbL film growth monitored by the UV−vis spectroscopy and circular dichroism spectra were reported. This material is available free of charge via the Internet at http://pubs.acs.org/.

AUTHOR INFORMATION

Corresponding Author

*E-mail: marystela@ufscar.br. Phone: +55 15 3229 5969.

Notes

The authors declare no competing financial interest.

ACKNOWLEDGMENTS

This work was supported by FAPESP (2012/16158-0), CNPq, CAPES, and nBioNet network (Brazil).

REFERENCES

(1) Gänzle, M. G.; Haase, G.; Jelen, P. Lactose: Crystallization, Hydrolysis, and Value-Added Derivatives. *Int. Dairy J.* **2008**, *18*, 685−694.

(2) Conzuelo, F.; Gamella, M.; Campuzano, S.; Ruiz, M. A.; Reviejo, A. J.; Pingarrón, J. M. An Integrated Amperometric Biosensor for the Determination of Lactose in Milk and Dairy Products. *J. Agric. Food Chem.* **2010**, *58*, 7141−7148.

(3) Shapiro, F.; Shamay, A.; Silanikove, N. Determination of Lactose and D-Galactose Using Thio-NAD+ instead of NAD+. *Int. Dairy J.* **2002**, *12*, 667−669.

(4) Harris, W. M. Automated Determination of Fat, Crude Protein, and Lactose in Ewe Milk by Infrared Spectrometry. *Analyst* **1986**, *111*, 37−39.

(5) Folin, O.; Denis, W. The Determination of Lactose in Milk. *J. Biol. Chem.* **1918**, *33*, 521−524.

(6) Xinmin, W.; Ruili, Z.; Zhihua, L.; Yuanhong, W.; Tingfu, J. Determination of Glucosamine and Lactose in Milk-Based Formulae by High-Performance Liquid Chromatography. *J. Food Compos. Anal.* **2008**, *21*, 255−258.

(7) Druzian, J. I.; Doki, C.; Scamparini, A. R. Simultaneous Determination of Sugars and Polyols in Low Calorie Ice Creams (diet/light) by High Performance Liquid Chromatography (HPLC). *Food Sci. Technol.* **2005**, *25*, 279−284.

(8) Pilloton, R.; Mascini, M. Flow Analysis of Lactose and Glucose in Milk with an Improved Electrochemical Biosensor. *Food Chem.* **1990**, *36*, 213−222.

(9) Marrakchi, M.; Dzyadevych, S. V.; Lagarde, F.; Martelet, C.; Jaffrezic-Renault, N. Conductometric Biosensor Based on Glucose Oxidase and β-Galactosidase for Specific Lactose Determination in Milk. *Mater. Sci. Eng., C* **2008**, *28*, 872−875.

(10) Göktuğ, T.; Sezgintürk, M. K.; Dinçkaya, E. Glucose Oxidase-β-Galactosidase Hybrid Biosensor Based on Glassy Carbon Electrode Modified with Mercury for Lactose Determination. *Anal. Chim. Acta* **2005**, *551*, 51−56.

(11) Fornera, S.; Yazawa, K.; Walde, P. Spectrophotometric Quantification of Lactose in Solution with a Peroxidase-Based Enzymatic Cascade Reaction System. *Anal. Bioanal. Chem.* **2011**, *401*, 2307−2310.

(12) Ferreira, M.; Fiorito, P. A.; Oliveira, O. N.; Córdoba de Torresi, S. I. Enzyme-Mediated Amperometric Biosensors Prepared with the Layer-by-Layer (LbL) Adsorption Technique. *Biosens. Bioelectron.* **2004**, *19*, 1611−1615.

(13) Ariga, K.; Ji, Q.; Mori, T.; Naito, M.; Yamauchi, Y.; Abe, H.; Hill, J. P. Enzyme Nanoarchitectonics: Organization and Device Application. *Chem. Soc. Rev.* **2013**, *42*, 6322−6345.

(14) Ricci, F.; Palleschi, G. Sensor and Biosensor Preparation, Optimization, and Applications of Prussian Blue Modified Electrodes. *Biosens. Bioelectron.* **2005**, *21*, 389−407.

(15) Campàs, M.; O'Sullivan, C. Layer-by-Layer Biomolecular Assemblies for Enzyme Sensors, Immunosensing, and Nanoarchitectures. *Anal. Lett.* **2003**, *36*, 2551−2569.

(16) Calvo, E. J.; Wolosiuk, A. Supramolecular Architectures of Electrostatic Self-Assembled Glucose Oxidase Enzyme Electrodes. *ChemPhysChem* **2004**, *5*, 235−239.

(17) Cui, A.; Tang, J.; Li, W.; Wang, Z.; Sun, C.; Zhao, M. Preparation of Catalytically Active Enzyme Thin Film by Alternate Deposition of Horseradish Peroxidase and Bipolar Quaternary Ammonium on Solid Surface. *Mater. Chem. Phys.* **2001**, *71*, 23−27.

(18) Ariga, K.; Yamauchi, Y.; Rydzek, G.; Ji, Q.; Yonamine, Y.; Wu, K. C.-W.; Hill, J. P. Layer-by-Layer Nanoarchitectonics: Invention, Innovation, and Evolution. *Chem. Lett.* **2014**, *43*, 36−68.

(19) Yan, Y.; Björnmalm, M.; Caruso, F. Assembly of Layer-by-Layer Particles and Their Interactions with Biological Systems. *Chem. Mater.* **2014**, *26*, 452−460.

(20) Hamlin, R. E.; Dayton, T. L.; Johnson, L. E.; Johal, M. S. A QCM Study of the Immobilization of β-Galactosidase on Polyelectrolyte Surfaces: Effect of the Terminal Polyion on Enzymatic Surface Activity. *Langmuir* **2007**, *23*, 4432−4437.

(21) Souza, T. T. L.; Moraes, M. L.; Ferreira, M. Use of Hemoglobin as Alternative to Peroxidases in Cholesterol Amperometric Biosensors. *Sens. Actuators, B* **2013**, *178*, 101−106.

(22) Widmer, F.; Leuba, J.-L. β-Galactosidase from Aspergillus Niger. *Eur. J. Biochem.* **1979**, *100*, 559−567.

(23) Zou, Y.; Xiang, C.; Sun, L.; Xu, F. Amperometric Glucose Biosensor Prepared with Biocompatible Material and Carbon Nanotube by Layer-by-Layer Self-Assembly Technique. *Electrochim. Acta* **2008**, *53*, 4089−4095.

(24) Bankar, S. B.; Bule, M. V.; Singhal, Rekha S.; Ananthanarayan, L. Glucose Oxidase—An Overview. *Biotechnol. Adv.* **2009**, *27*, 489−501.

(25) Lupu, S.; Mihailciuc, C.; Pigani, L.; Seeber, R.; Totir, N.; Zanardi, C. Electrochemical Preparation and Characterisation of Bilayer Films Composed by Prussian Blue and Conducting Polymer. *Electrochem. Commun.* **2002**, *4*, 753−758.

(26) Petri, L.; Ferreira, M.; Moraes, M. L. Toward Preserving the Structure of the Antigenic Peptide p17−1 from the HIV-1 p17 Protein in Nanostructured Films. *J. Nanosci. Nanotechnol.* **2011**, *11*, 6705−6709.

(27) Shen, Y. R. Surfaces Probed by Nonlinear Optics. *Surf. Sci.* **1994**, *299−300*, 551−562.

(28) Lambert, A. G.; Davies, P. B.; Neivandt, D. J. Implementing the Theory of Sum Frequency Generation Vibrational Spectroscopy: A Tutorial Review. *Appl. Spectrosc. Rev.* **2005**, *40*, 103−145.

(29) Zhang, D.; Zhang, K.; Yao, Y. L.; Xia, X. H.; Chen, H. Y. Multilayer Assembly of Prussian Blue Nanoclusters and Enzyme-Immobilized Poly(toluidine blue) Films and Its Application in Glucose Biosensor Construction. *Langmuir* **2004**, *20*, 7303−7307.
(30) Lakowicz, J. R. *Principles of Fluorescence Spectroscopy;* Springer: New York, N.Y., 2006.
(31) Muga, A.; Arrondo, J. L. R.; Bellon, T.; Sancho, J.; Bernabeu, C. Structural and Functional Studies on the Interaction of Sodium Dodecyl Sulfate with B-Galactosidase. *Arch. Biochem. Biophys.* **1993**, *300*, 451−457.
(32) Nguyen, J.; Baldwin, M. A.; Cohen, F. E.; Prusiner, S. B. Prion Protein Peptides Induce α-Helix to β-Sheet Conformational Transitions. *Biochemistry (Moscow, Russ. Fed.)* **1995**, *34*, 4186−4192.
(33) Cerf, E.; Sarroukh, R.; Tamamizu-Kato, S.; Breydo, L.; Derclaye, S.; Dufrêne, Y. F.; Narayanaswami, V.; Goormaghtigh, E.; Ruysschaert, J.; Raussens, V. Antiparallel β-Sheet: A Signature Structure of the Oligomeric Amyloid β-Peptide. *Biochem. J.* **2009**, *421*, 415−423.
(34) Liu, Y.; Ogorzalek, T. L.; Yang, P.; Schroeder, M. M.; Marsh, E. N. G.; Chen, Z. Molecular Orientation of Enzymes Attached to Surfaces through Defined Chemical Linkages at the Solid−Liquid Interface. *J. Am. Chem. Soc.* **2013**, *135*, 12660−12669.
(35) Ohto, U.; Usui, K.; Ochi, T.; Yuki, K.; Satow, Y.; Shimizu, T. Crystal Structure of Human Galactosidase: Structural Basis of G_{m1} Gangliosidosis and Morquio B Diseases. *J. Biol. Chem.* **2011**, *287*, 1801−1812.
(36) Arrondo, J. R. L.; Muga, A.; Castresana, J.; Bemabeu, C. An Infrared Spectroscopic Study of β-Galactosidase Structure in Aqueous Solutions. *FEBS Lett.* **1989**, *252*, 118−120.
(37) Matthews, B. W. The Structure of E. Coli β-Galactosidase. *C. R. Biol.* **2005**, *328*, 549−556.
(38) Ouyang, W.; Appelhans, D.; Voit, B.; Muller, M. Preparation and Enantiospecific Binding of Chiral Polyelectrolyte Multilayers: An in Situ ATR-FTIR Study. *Macromol. Symp.* **2007**, *254*, 180−187.
(39) Kim, H.; Urban, M. W. Reactions of Thrombresistant Multilayered Thin Films on Poly(vinyl chloride) (PVC) Surfaces: A Spectroscopic Study. *Langmuir* **1998**, *14*, 7235−7244.
(40) Vinhola, L.; Facci, T.; Dias, L. G.; Azevedo, D. C.; de Borissevitch, G.; Huguenin, F. Self-Assembled Films from Chitosan and Poly(vinyl sulfonic acid) on Nafion® for Direct Methanol Fuel Cell. *J. Braz. Chem. Soc.* **2012**, *23*, 531−537.
(41) Lvov, Y.; Decher, G.; Moehwald, H. Assembly, Structural Characterization, and Thermal Behavior of Layer-by-Layer Deposited Ultrathin Films of Poly(vinyl sulfate) and Poly(allylamine). *Langmuir* **1993**, *9*, 481−486.
(42) Decher, G. Fuzzy Nanoassemblies: Toward Layered Polymeric Multicomposites. *Science* **1997**, *277*, 1232−1237.
(43) Colthup, N. B.; Daly, L. H.; Wiberley, S. E. *Introduction to Infrared and Raman Spectroscopy;* 3rd ed.; Academic Press: Boston, MA, 1990.
(44) Adochitei, A.; Drochioiu, G. Rapid Characterization of Peptide Secondary Structure by FT-IR Spectroscopy. *Rev. Roum Chim* **2011**, *56*, 783−791.
(45) Clark, A. h.; Saunderson, D. h. p.; Suggett, A. Infrared and Laser-Raman Spectroscopic Studies of Thermally-Induced Globular Protein Gels. *Int. J. Pept. Protein Res.* **1981**, *17*, 353−364.
(46) Silva, H. S.; Uehara, T. M.; Bergamaski, K.; Miranda, P. B. Molecular Ordering in Layer-by-Layer Polyelectrolyte Films Studied by Sum-Frequency Vibrational Spectroscopy: The Effects of Drying Procedures. *J. Nanosci. Nanotechnol.* **2008**, *8*, 3399−3405.
(47) Harp, G.; Rangwalla, H.; Li, G.; Yeganeh, M.; Dhinojwala, A. Coupling of Interfacial Motion at Polystyrene−Alkane Interfaces. *Macromolecules* **2006**, *39*, 7464−7466.
(48) Opdahl, A.; Somorjai, G. A. Solvent Vapor Induced Ordering and Disordering of Phenyl Side Branches at the Air/Polystyrene Interface Studied by SFG. *Langmuir* **2002**, *18*, 9409−9412.
(49) Carvalho, N. M.; Pires, B. M.; Antunes, O. A.; Faria, R. B.; Osório, R. E.; Piovezan, C.; Neves, A. Use Of Equations Michaelis-Menten Parameters. *Quim. Nova* **2010**, *33*, 1607−1611.
(50) Wong, D. E.; Talbert, J. N.; Goddard, J. M. Layer by Layer Assembly of a Biocatalytic Packaging Film: Lactase Covalently Bound to Low-Density Polyethylene. *J. Food Sci.* **2013**, *78*, E853−E860.
(51) Klein, M. P. Immobilization of β-Galactosidase to Obtain Dairy Products with Content of Lactose. Dissertation, Federal University of Rio Grande do Sul: Porto Alegre, Brazil, 2010.
(52) Ansari, S. A.; Satar, R.; Alam, F.; Alqahtani, M. H.; Chaudhary, A. G.; Naseer, M. I.; Karim, S.; Sheikh, I. A. Cost Effective Surface Functionalization of Silver Nanoparticles for High Yield Immobilization of Aspergillus Oryzae β-Galactosidase and Its Application in Lactose Hydrolysis. *Process Biochem.* **2012**, *47*, 2427−2433.
(53) Rejikumar, S.; Devi, S. Hydrolysis of Lactose and Milk Whey Using a Fixed-Bed Reactor Containing β-Galactosidase Covalently Bound onto Chitosan and Cross-Linked Poly(vinyl alcohol). *Int. J. Food Sci. Technol.* **2001**, *36*, 91−98.
(54) Ammam, M.; Fransaer, J. Two-Enzyme Lactose Biosensor Based on β-Galactosidase and Glucose Oxidase Deposited by AC-Electrophoresis: Characteristics and Performance for Lactose Determination in Milk. *Sens. Actuators, B* **2010**, *148*, 583−589.